# Calibration Evaluation and Radiometric Testing of Field Radiometers with the SeaWiFS Quality Monitor (SQM)

STANFORD B. HOOKER

*NASA/Goddard Space Flight Center, Laboratory for Hydrospheric Processes, Greenbelt, Maryland*

JAMES AIKEN

*Plymouth Marine Laboratory, Plymouth, United Kingdom*

(Manuscript received 21 March 1997, in final form 4 September 1997)

ABSTRACT

One of the goals of calibration and validation programs supporting ocean color satellites is to produce water-leaving radiances with an uncertainty of 5% in clear-water regions. This objective requires field instruments with a calibration and measurement capability that is on the order of 1%. The Sea-viewing Wide Field-of-view Sensor (SeaWiFS) Project, in collaboration with the National Institute of Standards and Technology, has developed a portable illumination source with three temperature-stabilized internal monitors designed to provide a stable light field for checking the optical stability of radiometers used to measure the in situ optical properties of seawater. This device is called the SeaWiFS Quality Monitor (SQM). A recent field evaluation during an extensive research cruise indicates the SQM has the following capabilities: (a) the SQM can be used to track the stability of field radiometers at less than the 1% level in terms of the radiometric response of the instruments—on average 0.30% (±0.15%) for radiance sensors and 0.58% (±0.20%) for irradiance sensors; (b) the SQM light field is sufficiently stable to allow for a sensitive measure and, thus, modeling of changes in the radiometric detectors; (c) based on the radiometers used during the field evaluation, daily SQM measurements are needed to resolve the temporal changes in the response of the sensors; and (d) SQM performance, in terms of the generated light field and the SQM internal monitors, is very stable and decayed only by approximately 0.6% during the course of the 36-day deployment with most of the decay attributed to a change in the operating voltage of one of the lamps.

## 1. Introduction

The Sea-viewing Wide Field-of-view Sensor (SeaWiFS) was designed as the successor ocean color satellite to the *Nimbus-7* Coastal Zone Color Scanner (CZCS), which ceased operation in 1986 after more than seven years of operation. Unlike the CZCS sensor, which was planned as a proof-of-concept instrument, the SeaWiFS instrument is designed to provide routine global coverage every two days for a 5-yr lifetime and to provide estimates of photosynthetic pigment concentrations of sufficient accuracy for use in quantitative studies of the ocean's primary productivity and biogeochemistry (Hooker and Esaias 1993). One of the primary goals of the SeaWiFS calibration and validation program is to produce water-leaving radiance, $L_w$, estimates with an uncertainty of 5% in clear-water regions (McClain et al. 1992).

The SeaWiFS in situ radiometric objectives require field instruments with a calibration and measurement uncertainty on the order of 1%. In the absence of a portable illumination source, scientists deploying radiometers to the field can at best calibrate their instruments before and after field campaigns and, under most circumstances, rely on annual or biannual calibrations. With this kind of calibration scenario, changes in instrument performance are necessarily assumed to be linear, which is obviously an optimistic assumption. In an effort to correct this deficiency in deployment and calibration practices, the SeaWiFS Project, in collaboration with the National Institute of Standards and Technology, has developed the SeaWiFS Quality Monitor (SQM), a portable, computer-controlled illumination source.

The SQM was designed to provide a stable light field for checking the radiometric stability of radiometers used to measure the in situ optical properties of seawater while they are being deployed in the field. The engineering design and characteristics of the SQM are described by Shaw et al. (1997) and Johnson et al. (1998), so only a brief description is given here. A separate rack of electronic equipment, composed principally of two computer-controlled power supplies and a digital multimeter, are an essential part of producing the stable light

*Corresponding author address:* Dr. Stanford B. Hooker, NASA/Goddard Space Flight Center, Greenbelt, MD 20771.
E-mail: stan@ardbeg.gsfc.nasa.gov

field. The SQM does not have, nor does it require, an absolute calibration, but it has design objectives of better than 2% stability during field deployments.

The SQM has two sets of subminiature halogen lamps with eight lamps in each set; both lamp sets are arranged symmetrically on a ring and operate in series, so if one lamp fails, the entire set goes off. The lamps in one set are rated for 1.05 A (4.2 V) and are operated at 0.95 A, and the lamps in the other set are rated for 3.45 A (5.0 V) and are operated at 3.1 A; the lamp sets are hereafter referred to as the 1-A and 3-A lamps, respectively. The lamps are operated at approximately 90% of their full amperage rating to maximize the lifetime of the lamps.

A low (*L*), medium (*M*), or high (*H*) intensity is provided when the 1-A, 3-A, or both lamp sets are used, respectively. Each lamp set was *aged* for approximately 50 h before deploying the SQM to the field. The interior light chamber has bead-blasted aluminum walls, so the diffuse component of the reflectance is significant. The lamps illuminate a circular plastic diffuser that is resilient to ultraviolet yellowing but can age nonetheless. The diffuser is protected by safety glass, which is sealed from the environment by o-rings. The exit aperture is 20 cm in diameter and has a spatial uniformity of 98% or more over the interior 15-cm circle.

A faceplate or *shadow collar* provides a mounting assembly, so the device under test (DUT), usually a radiance or irradiance sensor, can be positioned in the shadow collar. The DUT has a D-shaped collar fitted to it at a set distance, 3.81 cm (1.5 in.), from the front of the DUT. This distance was chosen based on the most restrictive clearance requirement of the radiometers used in the different field deployment rigs. The D-shaped collar ensures that the DUT can be mounted to the SQM at a reproducible location and orientation with respect to the exit aperture each time the DUT is used. The former minimizes uncertainties (principally with irradiance sensors) due to distance differences between measurement sessions, while the latter minimizes uncertainties (principally with radiance sensors) due to inhomogeneities in the exit aperture light field. In either case, the D-shaped collar keeps these sources of uncertainties below the 1% level.

The SQM faceplate can be changed to accept a variety of instruments from different manufacturers. Radiometers above a certain size, approximately 15 cm, would obviously be difficult to accommodate, but the entire mounting assembly can be changed to allow for reasonable viewing by seemingly difficult-to-handle devices. To date, three radiometer designs have been used with the SQM, and there were no problems in producing the needed faceplates, D-shaped collars, or support hardware to accommodate these units.

The SQM light field can change due to one or more of a variety of effects, for example, the presence of the DUT, the aging of the lamps, a deterioration in the plastic diffuser, a change in the transmittance of the glass cover, a drift in the control electronics, a repositioning of a mechanical alignment, etc. To account for these changes, three photodiodes, whose temperatures are kept constant with a thermoelectric cooler, measure the exit aperture light level: the first has a responsivity in the blue part of the spectrum, the second in the red part of the spectrum, and the third has a broadband or *white* response. All three internal monitors view the center portion of the exit aperture. The back of the SQM is cooled by a multispeed fan to prevent a buildup in temperature beyond what the thermoelectric cooler can accommodate (the lower fan speed settings are used to prevent overcooling of the SQM in cold climates). The SQM has an internal heater to help maintain temperature stability in colder climates and to shorten the time needed for warming up the SQM.

Another SQM quality control procedure is provided by three special DUTs called *fiducials*: a white one, a black one, and a black one with a glass face (the glass is the same as that used with the field radiometers). A fiducial has the same size and shape of a radiometer but is nonoperational. The reflective surface of a fiducial is carefully maintained, both during its use and when it is not being used. Consequently, the reflective surface degrades very slowly, so over the time period of a field expedition, it remains basically constant. A field radiometer, by comparison, has a reflective surface that is changing episodically because of the wear and tear of daily use. This change in reflectivity alters the loading of the radiometer on the SQM and is a source of variance for the monitors inside the SQM that are viewing the exit aperture or the radiometer itself when it is viewing the exit aperture. The time series of a fiducial, as measured by the SQM internal monitors, gives an independent measure of the temporal stability of the SQM light field.

This paper describes the field evaluation of the SQM during an extensive research cruise on the Royal Research Ship *James Clark Ross.* The paper is organized into separate descriptions of the field expedition, the methodology for collecting SQM data, the analytical approach taken to analyze the data, the results of the data analysis, and an evaluation of the capabilities of the SQM based on the results achieved.

## 2. Field commissioning

Twice a year, the *James Clark Ross* steams an Atlantic meridional transect (AMT) between Grimsby, United Kingdom, and Stanley, Falkland Islands, with a port call in Montevideo, Uruguay. The latitudinal range of the transect, in terms of the in situ sampling, is approximately 50°N–50°S. The AMT cruises are designed to provide spatially extensive calibration and validation data for satellite ocean color sensors (Robins and Aiken 1996). During the third AMT cruise, AMT-3, which was in September and October 1996, three different multispectral profilers were deployed: 1) the SeaWiFS Op-

tical Profiling System (SeaOPS), 2) the Undulating Oceanographic Recorder (UOR), and 3) the SeaWiFS Free-Falling Advanced Light Level Sensors (SeaFALLS). All of the light sensors used with these systems, including any spares, were filter radiometers manufactured by Satlantic, Inc. (Halifax, Canada). This commonality in equipment was not by accident; the AMT scientists felt this was the easiest way to ensure redundancy and easy intercalibration.

SeaOPS is composed of an above-water and in-water set of instruments (Robins et al. 1996). The in-water component is composed of a downward-looking radiance sensor (OCR-200), which measures upwelling radiance, $L_u$, and an upward-looking irradiance sensor (OCI-200), which measures downwelling irradiance, $E_d$. The in-water instruments are mounted on a T-shaped frame that is lowered and raised through the water column by a winch. The frame is suspended from the end of a boom that extends approximately 10 m from the side of the ship, and the data are collected during the lowering and raising of the frame. The above-water component, an OCI-200, measures the incident solar irradiance at the ocean surface, $E_d^+$. The OCI-200 and OCR-200 radiometers have seven channels that were chosen to correspond to the SeaWiFS instrument wavelengths and bandwidths (Hooker et al. 1993).

The UOR is a measurement platform that is towed approximately 400 m behind a ship (Aiken and Bellan 1990), where the wake effects of the ship's passage are usually substantially reduced. It uses a programmable servo that controls the attitude of a diving plane, which causes the vehicle to undulate through a preset depth range, typically 5–75 m, at tow speeds between 10 and 12 kt. At speeds in excess of 6 kt, the servo unit is powered by an alternator, which is driven by a propeller on the rear of the body. During AMT-3, an OCI-200 was fitted to the top of the UOR instrument bay to measure $E_d$ and an OCR-200 was fitted to the bottom of the instrument bay to measure $L_u$. The OCI-200 and OCR-200 radiometers employed in the UOR and SeaOPS use 16-bit A/D convertors and are capable of detecting light over a four-decade range.

SeaFALLS is composed of two subsystems: a SeaWiFS Profiling Multichannel Radiometer and a SeaWiFS Multichannel Surface Reference. The former measures $E_d$ and $L_u$ as it falls freely through the water column, and the latter measures the incident solar irradiance just below the sea surface, $E_d^-$. The profiler receives its power and sends its data via an umbilical cable, whereas the reference floats just below the surface suspended from a square floating frame (Waters et al. 1990). Both the profiler and the reference can be deployed far away (greater than 30 m) from the ship, so any ship-induced disturbances to the in situ light field are minimized (Mueller and Austin 1995). SeaFALLS is equipped with 13-channel OCI-1000 and OCR-1000 radiometers, which employ 24-bit A/D convertors and are capable of detecting light over a seven-decade range.

Two different types of detectors were involved with the SQM field test. The first type was the three photodiodes inside the SQM that monitor the SQM flux, and the second type was the various radiometers whose radiometric stability was checked by having them view the SQM aperture while positioned in the shadow collar. The radiometers fall into different usage categories based on whether or not the optical systems had primary and secondary sensors. Primary sensors were always deployed into the ocean if they were functioning properly, whereas secondary sensors, which were taken along as backups or spares, were deployed only if a primary sensor failed. This proved to be an important redundancy; approximately three-fourths of the way through the cruise, the UOR primary irradiance sensor failed because of a bad bulkhead connector (the pins failed prematurely because of a manufacturing defect) and was replaced with its secondary sensor.

With respect to the SQM sessions, eight radiometers were used frequently (more than 15 times) and four were used only occasionally (5 times). The former involved radiometers that were easily reconfigured for use with the SQM—that is, they could be permanently fitted with an SQM D-shaped collar and quickly removed from their deployment rigs (SeaOPS and UOR); whereas, the latter involved deployment rigs that had to be significantly disassembled before the radiometer could be used with the SQM (SeaFALLS). This difference highlights an important aspect of using the SQM with existing equipment that could not have envisioned the use of the SQM as part of the normal deployment strategy: some redesign may be needed to ensure an easily executed methodology. Unfortunately, in this case, three of the four less frequently used radiometers were the radiometers with the best sampling precision (24-bit A/D convertors) and spectral discrimination (13 channels).

## 3. Methodology

On the AMT-3 cruise, the SQM was sited in the so-called *rough workshop* on the main deck adjacent to the aft working space from where the optical profilers were deployed. The workshop was moderately well temperature controlled: air conditioned to approximately 20°C in the equatorial zones and heated to about 18°C in higher latitudes. Nonetheless, the room was subjected to periodic swings in temperature as a consequence of normal deck operations. These changes in temperature were particularly noticeable in the final leg of the voyage between Montevideo and Stanley when the outside air temperature was the coldest.

To check the stability of the radiometers used during AMT-3, and to monitor the performance of the SQM, a calibration evaluation and radiometric testing (CERT) session was defined. A sequence of procedures was implemented for each CERT session (with minor variations to test SQM performance aspects or to accommodate equipment and scheduling problems).

TABLE 1. A summary of the DUTs used during AMT-3. For some of the optical systems, a primary (frequently deployed into the ocean), and secondary (backup), sensor was available. The DUT code is composed of a single letter device code and a two-digit serial number. The right-most columns indicate the number of CERT sessions each DUT was used in.

| Optical system | DUT model | Physical measure | DUT serial number | | DUT code | | CERT sessions | |
|---|---|---|---|---|---|---|---|---|
| | | | Primary | Secondary | Primary | Secondary | Primary | Secondary |
| SeaOPS | OCI-200 | $E_d$ | 29 | 40 | I29 | I40 | 21 | 18 |
| | OCR-200 | $L_u$ | 21 | 35 | R21 | R35 | 20 | 19 |
| | OCI-200 | $E_d^+$ | 30 | | M30 | | 5 | |
| UOR | OCI-200 | $E_d$ | 1 | 2 | I01 | I02 | 12 | 17 |
| | OCR-200 | $L_u$ | 1 | 2 | R01 | R02 | 17 | 18 |
| SeaFALLS | OCI-1000 | $E_d$ | 23 | | H23 | | 5 | |
| | OCR-1000 | $L_u$ | 16 | | Q16 | | 5 | |
| | OCI-1000 | $E_d^-$ | 24 | | H24 | | 5 | |
| SQM | SBF | | 1 | | B01 | | 13 | |
| | SGF | | 1 | | G01 | | 22 | |
| | SWF | | 1 | | W01 | | 14 | |

1) The rack of electronics equipment (the lamp power supplies and the digital multimeter, the SQM fan and internal heater power supplies, the lamp timers, and the thermoelectric cooler controller) were turned on 1–2 h before the CERT session was to begin. In addition, the total number of hours on each lamp set was tracked by recording the starting and ending number of hours on each lamp set.
2) The SQM was preheated using the internal electrical heater for 30–60 min, depending on the environmental conditions at the time. This was done to achieve a time-efficient thermal equilibrium of the instrument from the power dissipation of the lamps.
3) One radiometer, most frequently the primary SeaOPS radiance sensor, was selected to monitor the warming up, and occasionally the powering up, of the SQM. The first data collected during the CERT session were the dark voltages for this radiometer, which was achieved by putting an opaque cap on the radiometer and collecting data for 3 min.
4) Once the SQM was powered up at the selected lamp level, it was allowed to warm up for at least 1 h, and frequently for as long as 2 h. During this time, the environmental temperature, lamp voltages, and internal temperatures of the SQM were recorded. The warm-up period was deemed completed when the internal SQM monitors achieved a constant value to within 0.05%. The radiometric stability usually coincided with a thermal equilibrium as denoted by the internal thermistors.
5) Upon the completion of the warm-up period, the individual radiometric sensors were tested sequentially. First, the previous DUT was removed and replaced with a glass fiducial. Second, dark voltages for the radiometer to be tested and SQM monitor data for the glass fiducial were simultaneously collected for 3 min. Third, the glass fiducial was removed from the SQM and replaced with the radiometer. Finally, data from the SQM and the radiometer were recorded for 3 min. Each time a DUT was mounted to the SQM for 3 min, the lamp voltages and internal temperatures of the SQM were recorded. Each data collection event (lasting 3 min) is referred to here as a data acquisition sequence (DAS) and represents approximately 1080 radiometer samples and 15 SQM (internal monitor) samples.
6) Before the SQM was shut down, the remaining white and black fiducials were measured. These measurements, plus the fiducial data acquired using the glass fiducial in between radiometer dark and light (SQM) measurements, are the primary sources for tracking the stability of the SQM flux. In some cases, a radiometer recorded the powering down of the lamps. After the lamps were powered down, the ending number of hours on each lamp set was recorded.

It is important to note the warm-up process involved only the SQM, and it was done only once before the individual DUTs were measured; the DUTs were not warmed up per se, although, they were kept in the same room as the SQM, so they were at room temperature.

The point for radiometric stability of the internal SQM monitors (0.05%) was usually achieved within 30–90 min of powering up the lamps, depending on the amount of preheating. In general, the warm-up period was extended another 30 min past this point to ensure that stability could be maintained. The radiometric stability of the SQM immediately after powering on the lamps (i.e., within 1 min) was usually less than 0.2% with preheating, and as much as 2% without preheating, depending on the environmental conditions. If a radiometer was subjected to some kind of trauma and needed to be checked as quickly as possible for an impending deployment, it would be possible to check it to within reasonable limits using a rapid start of the SQM, particularly if the SQM was kept in a preheated mode.

The models and serial numbers of the DUTs are presented in Table 1 along with the number of CERT sessions each was used in. The center wavelengths for the radiometer channels, as supplied by the manufacturer, are given in Table 2. The radiometers have very similar channels, so they can be grouped by channel number

TABLE 2. Channel numbers and center wavelengths (nm) for the radiometers used during AMT-3. All of the channels have 10-nm bandwidths.

| Channel number | SeaOPS | | | | | UOR | | | | SeaFALLS | | |
|---|---|---|---|---|---|---|---|---|---|---|---|---|
| | I29 | R21 | M30 | I40 | R35 | I01 | R01 | I02 | R02 | H23 | Q16 | H24 |
| 1 | 413.0 | 411.1 | 411.3 | 411.5 | 411.1 | 412.3 | 411.9 | 412.8 | 412.0 | 405.9 | 406.2 | 406.3 |
| 2 | 443.2 | 443.6 | 442.3 | 442.5 | 442.9 | 442.4 | 442.5 | 442.5 | 443.0 | 412.3 | 412.8 | 411.6 |
| 3 | 490.5 | 489.5 | 490.5 | 489.5 | 489.9 | 490.1 | 489.9 | 490.1 | 489.8 | 665.9 | 665.0 | 665.7 |
| 4 | 509.2 | 509.2 | 509.2 | 509.6 | 509.7 | 509.9 | 509.7 | 509.9 | 509.1 | 443.5 | 443.1 | 443.9 |
| 5 | 555.5 | 555.4 | 555.0 | 555.2 | 555.0 | 555.6 | 555.4 | 555.8 | 555.6 | 470.4 | 470.6 | 469.9 |
| 6 | 665.6 | 665.7 | 664.8 | 664.9 | 665.5 | 670.4 | 669.8 | 664.9 | 669.7 | 490.6 | 490.6 | 490.6 |
| 7 | 683.8 | 683.2 | 682.6 | 683.5 | 683.7 | 700.1 | 682.5 | 683.5 | 682.5 | 509.4 | 509.3 | 509.5 |
| 8 | | | | | | | | | | 532.8 | 532.9 | 532.6 |
| 9 | | | | | | | | | | 555.1 | 555.2 | 555.2 |
| 10 | | | | | | | | | | 589.9 | 589.8 | 590.0 |
| 11 | | | | | | | | | | 670.5 | 670.4 | 670.5 |
| 12 | | | | | | | | | | 683.7 | 682.7 | 683.6 |
| 13 | | | | | | | | | | 700.3 | 700.4 | 700.6 |

for the purpose of (statistically) describing their performance as measured by the SQM.

The AMT-3 cruise began on 20 September and ended on 25 October, a total of 36 days. During that time, a short system functionality test and 21 regular CERT sessions were executed. The initial functionality test verified there were no problems as a result of shipping the SQM. For the purposes of presenting the data, the sequential day of the year (SDY) is used to denote the daily cruise timeline (20 September is SDY 264 and 25 October is SDY 299). Most of the CERT sessions were conducted indoors in the rough workshop while the ship was under way, although some were conducted outdoors and others were conducted in port.

For the purposes of AMT-3, the SQM was considered an unproven instrument whose short- and long-term reliability was not known, so a cautious sampling strategy was adopted: the majority of the data were collected at the low lamp level. The higher lamp level and testing sessions were sporadically included to provide data on as diverse a suite of parameters as possible. Out of the 21 regular CERT sessions performed during AMT-3, 14, 3, and 4 were at the low, medium, and high SQM lamp levels, respectively.

For three CERT sessions, the SQM was operated outside (on a table) at ambient temperatures, ranging from 28°C in the Tropics to 15°C in Montevideo and south to Stanley. During the outdoor sessions, the SQM was shaded from direct sunlight and ambient wind conditions; for a limited amount of time, and only under controlled circumstances, the SQM was also used unshaded. In addition, three of the AMT-3 sessions were conducted in port during which the SQM was not subjected to ship roll and vibration (with the exception of the electric generators). The day before reaching Stanley, on SDY 298, the internal SQM heater was tested in a variety of configurations to determine the importance of the heater to measurements in cold climates (the fan was kept at a constant speed).

A summary of all the deployment information is presented in Table 3, which is an abbreviated version of the SQM master log corresponding to the AMT-3 cruise period. CERT sessions were also performed before and after the cruise, so a total of 23 regular CERT sessions compose the results presented here. The pre- and post-cruise use of the SQM was under more limited circumstances and are not summarized in Table 3. In the case of the former, the SQM was still being completed for its first field use, and for the latter, many of the radiometers were not readily available because some were being used in other measurement campaigns and others were being recalibrated in preparation for other uses.

## 4. Approach

Because of the variety of detectors and lamp levels, a compacted notation is used here to discuss the signals under consideration. In the most general terms, the quantity of interest is a voltage associated with a radiometer (or DUT), $V^C(\lambda_i, t_j)$, where $V$ is the voltage of the radiometer under illumination at the time of the measurement, $C$ is the instrument code of the DUT (Table 1), $\lambda_i$ is an individual wavelength or channel of the instrument, and $t_j$ is a particular time for a digitized record. Since the SQM has two different sets of lamps, there are three basic voltage levels for the SQM monitors and for the radiometers while they are mounted to the SQM: $L$, $M$, and $H$, which correspond to the low, medium, and high lamp levels, respectively. In addition, the radiometers acquired data while they were covered with an opaque cap and the detectors measured dark voltages ($D$). Unfortunately, the data acquisition software that controlled the SQM did not allow for the collection of dark values for the internal SQM monitors.

All of the data for a particular CERT session were acquired at a single lamp level. If the SQM data acquisition and control software failed during a CERT session, which occasionally happened, the software was restarted and the SQM was allowed to warm up until it reached thermal and electrical stability as measured by

TABLE 3. SQM master log summary for the time period corresponding to the AMT-3 cruise. The instrument location codes specify if the CERT sessions were conducted in port (*P*) or under way while at sea (*U*). All of the measurements were taken indoors in the rough workshop (*W*) or outdoors on deck (*O*). The internal SQM heater was tested in a variety of configurations on SDY 298; these tests were conducted in the rough workshop and are denoted by the *T* data code. The beginning and ending time when DUTs were being measured (after the SQM had been warmed up) is given in Greenwich Mean Time (GMT), but to keep time monotonic (for easy differencing), any DAS sessions that extended into the next GMT day have 2400 added to their ending times.

| Session number | GMT SDY | Data codes | | Beginning hours | | Lamps setting | DAS sessions | | Ending hours | |
|---|---|---|---|---|---|---|---|---|---|---|
| | | Motion | Location | 1A | 3A | | Begin | End | 1A | 3A |
| 0 | 262 | *P* | *W* | 47.04 | 80.22 | *H* | None | | 47.64 | 80.89 |
| 1 | 266 | *U* | *W* | 47.64 | 80.89 | *H* | 1625 | 1920 | 53.94 | 87.06 |
| 2 | 267 | *U* | *W* | 53.84 | 87.06 | *H* | None | | 56.74 | 89.98 |
| 3 | 268 | *U* | *W* | 56.74 | 89.98 | *H* | 2326 | 2447 | 61.29 | 94.59 |
| 4 | 271 | *U* | *W* | 61.29 | 94.59 | *L* | 2322 | 2438 | 64.54 | 94.59 |
| 5 | 272 | *U* | *W* | 64.54 | 94.59 | *M* | 2306 | 2512 | 64.54 | 98.42 |
| 6 | 274 | *U* | *W* | 64.54 | 98.42 | *L* | 2241 | 2421 | 68.01 | 98.42 |
| 7 | 276 | *U* | *W* | 68.01 | 98.42 | *L* | 2227 | 2446 | 71.57 | 98.42 |
| 8 | 278 | *U* | *W* | 71.57 | 98.42 | *L* | 2201 | 2314 | 74.08 | 98.42 |
| 9 | 280 | *U* | *W* | 74.08 | 98.42 | *L* | 2258 | 2411 | 77.06 | 98.42 |
| 10 | 282 | *U* | *O* | 77.06 | 98.42 | *L* | 1511 | 1540 | 83.52 | 98.42 |
| 11 | 283 | *U* | *W* | 83.52 | 98.42 | *M* | 2319 | 2432 | 83.52 | 101.49 |
| 12 | 284 | *U* | *O* | 83.52 | 101.49 | *M* | 1842 | 1901 | 83.52 | 105.06 |
| 13 | 286 | *U* | *W* | 83.52 | 105.06 | *L* | 2307 | 2526 | 87.04 | 105.06 |
| 14 | 289 | *U* | *W* | 87.04 | 105.06 | *L* | 2445 | 2554 | 89.96 | 105.06 |
| 15 | 292 | *P* | *W* | 89.96 | 105.06 | *L* | 1859 | 2102 | 93.28 | 105.06 |
| 16 | 293 | *P* | *O* | 93.28 | 105.06 | *H* | 1850 | 1858 | 95.95 | 107.92 |
| 17 | 296 | *U* | *W* | 95.95 | 107.92 | *L* | 2322 | 2425 | 99.23 | 107.92 |
| 18 | 297 | *U* | *W* | 99.23 | 107.92 | *L* | 2242 | 2341 | 102.34 | 107.92 |
| 19 | 298 | *U* | *T* | 102.34 | 107.92 | *L* | 1801 | 1845 | 104.54 | 107.92 |
| 20 | 298 | *U* | *T* | 104.54 | 107.92 | *L* | 1952 | 2048 | 106.48 | 107.92 |
| 21 | 299 | *P* | *W* | 106.48 | 107.92 | *L* | 1703 | 1856 | 110.47 | 107.92 |

the thermistors and lamp voltages. (No ill effects were seen in the data as a result of this practice.)

The process of determining a parameter for monitoring the radiometric stability of a radiometer during a field deployment begins by first defining the mean signal level acquired with the radiometer during a DAS:

$$\overline{V}^{C}(\lambda_i) = \frac{1}{n}\sum_{j=1}^{n} V^{C}(\lambda_i, t_j), \tag{1}$$

where $(\overline{\ })$ denotes a time average of the total number of samples, *n*, collected during a DAS (usually 1080). Dark readings were taken for each radiometer before they were mounted to the SQM. Following (1), the mean dark voltage for a DAS is defined as

$$\overline{D}^{C}(\lambda_i) = \frac{1}{n}\sum_{j=1}^{n} D^{C}(\lambda_i, t_j). \tag{2}$$

While the dark readings for a radiometer were being collected, a fiducial was placed inside the SQM and the signals from the internal SQM monitors were recorded. The voltages from the monitors are denoted by $X_S^C$, where *X* can be *L*, *M*, or *H*, depending on the selected SQM lamp level; *C* is the instrument code for the DUT in the SQM; and *S* indicates the internal monitor under consideration: *B* for the blue monitor, *R* for the red monitor, and *W* for the broadband or white monitor.

Changes in a radiometric signal can arise from changes in the light source, the digitization electronics, or the detector electronics. Tracking the performance of a radiometer over extended time periods must take into account these three influences on the signal. The basic parameter for tracking the radiometers deployed during AMT-3 is constructed by taking the mean voltage from the radiometer when it was mounted to the SQM, subtracting the mean dark voltage, and then normalizing the difference by one of the mean internal SQM monitor voltages:

$$\tilde{V}_S^C(\lambda_i, t_k) = \frac{\overline{V}^{C}(\lambda_i) - \overline{D}^{C}(\lambda_i)}{\overline{X}_S^C}, \tag{3}$$

where $(\tilde{\ })$ denotes a normalized result for a DAS, $t_k$ indicates the time period for the DAS, and *S* is used to denote the internal SQM monitor used for normalization: *B*, *R*, or *W*. Note that dark voltages should also be subtracted from the normalization signals, but this was not possible with the version of the SQM control software used during AMT-3. The uncertainty due to this omission was seen to be negligible because of the high quality of the multimeter that was used to digitize the SQM monitor signals (a multiplexed Hewlett Packard 3457A with 6.5 digits of precision). Within the uncertainties of the measurements, $\tilde{V}_S^C(\lambda_i)$ should be a constant from one CERT session to the next, since an increase (decrease) in SQM intensity should coincide with an increase (decrease) in the radiometer signal.

If *N* is the total number of CERT sessions at a particular lamp level, the mean normalized signal for a particular radiometer at that lamp level is given by

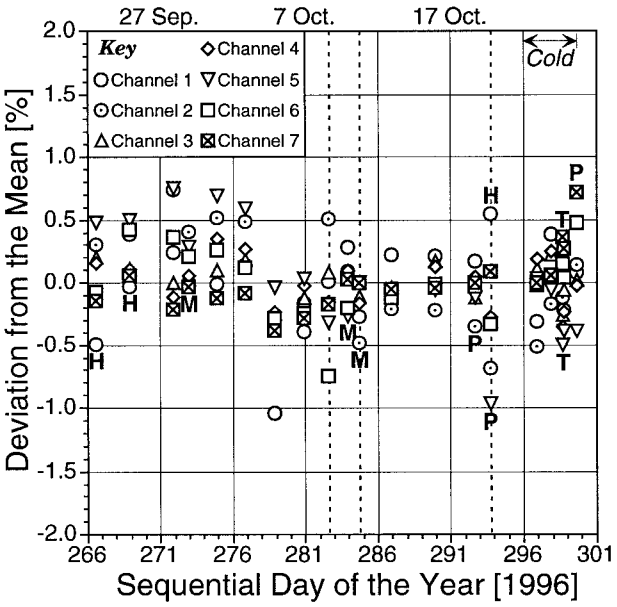


FIG. 1. A plot of $\check{V}_W^{R21}(\lambda_i)$ at the three lamp levels for the AMT-3 cruise. The measurements taken at the medium and high lamp levels are indicated by the M and H labels; all others are at the low lamp level. Those measurements taken in port are indicated by the P label; all others are taken while under way at sea. The measurements corresponding to the testing of the SQM internal heater south of Montevideo in cold weather are indicated by the T label. The dashed lines indicate measurements taken outdoors; all other measurements were taken indoors. The normalization in each case is with respect to the white SQM internal monitor. The center wavelengths for each channel are given in Table 2 and all times are in GMT.

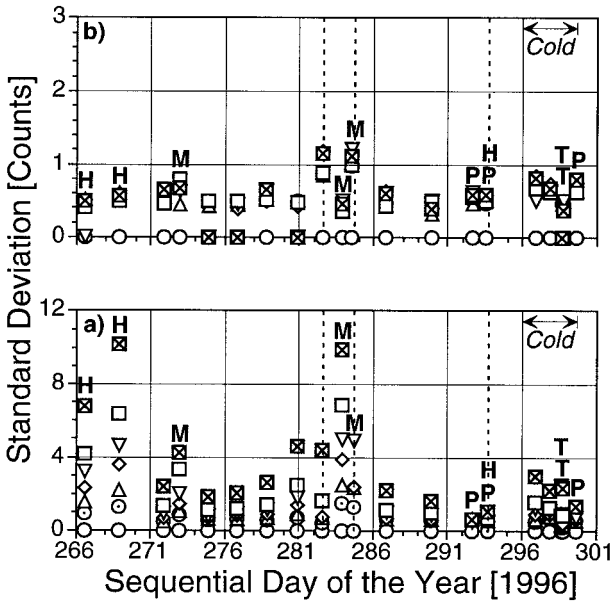


FIG. 2. The standard deviation of each channel voltage for radiometer R21 during the DAS events in Fig. 1 while it was (a) mounted to the SQM and (b) during dark data collection. The channel coding and event labeling is the same as for Fig. 1.

$$\hat{V}_S^C(\lambda_i) = \frac{1}{N}\sum_{k=1}^{N} \tilde{V}_S^C(\lambda_i, t_k), \tag{4}$$

where ($\hat{}$) denotes the mean of the normalized signals and $t_k$ represents a particular DAS time period.

The temporal performance of a radiometer is determined by calculating the percent deviation of the radiometer (during a particular DAS time, $t_k$) from the mean of all of the normalized signals (4):

$$\check{V}_S^C(\lambda_i, t_k) = 100\left[\frac{\tilde{V}_S^C(\lambda_i, t_k)}{\hat{V}_S^C(\lambda_i)} - 1\right], \tag{5}$$

where ($\check{}$) denotes the percent deviation of the normalized signals with respect to the mean for a particular lamp level, the mean being determined from the time series of data collected during a field deployment. Thus, $\check{M}_W^{R21}(412)$ is the percent deviation of the radiances for the 412-nm channel of radiometer OCR-200 serial number 21 (instrument code R21) at the medium lamp level normalized with the white SQM internal monitor.

## 5. Analysis

The primary purpose of the SQM is to determine the radiometric stability of a radiometer during a field deployment. The analysis of this capability begins with R21, one of the primary field radiometers used during AMT-3. Figure 1 is a plot of $\check{V}_W^{R21}(\lambda_i)$ at the three lamp levels for the entire cruise. Despite differences in lamp intensities, environmental conditions, and ship motion states, there are no obvious biases or trends in the data. Using the absolute values of the individual deviations, the mean percent deviation for all of the channels is 0.23, and the averages for the individual channels 1–7 are 0.26, 0.35, 0.13, 0.17, 0.33, 0.21, and 0.16, respectively. From an averaged and normalized perspective, then, radiometer R21 was stable to within $\pm 0.35\%$.

A closer inspection reveals some interesting aspects regarding the response of radiometer R21 during AMT-3. Figure 2a is a plot of the standard deviation ($\sigma$) in the R21 signal voltages while the radiometer was mounted to the SQM and during data collection for the DAS events in Fig. 1. The signal value was defined as the detector value minus the mean dark value, and the standard deviation values were calculated from the despiked signal data. The despiking employed was a $2\sigma$ filter—that is, any data that was $\pm 2\sigma$ from the mean signal level for the DAS was rejected; after filtering, a new signal mean and $\sigma$ was computed for the DAS. The new despiked values are reported in Fig. 2a. In general, very few spikes were encountered, but they do occur and need to be removed.

The Fig. 2a $\sigma$ values indicate higher deviations during less controlled environmental conditions, for example, when the SQM was used outdoors (dashed lines) while the ship was under way and windage was a problem. Sun loading and any sea spray were minimized by shading the top of the SQM with a piece of canvas, but the

canvas was ineffective against the swirling winds encountered on the rear deck of the ship where the measurements were taken. The outdoor standard deviations are on average about 31% larger than the indoor values. The importance of environmental effects is also seen in the variance of the dark data (Fig. 2b): the outdoor dark standard deviations are on average 90% higher than the indoor values, but they are small (on average less than 1 count) under all circumstances. This same effect of elevated variance in the outdoor CERT sessions is also seen in the SQM deck box (lamp voltages and internal temperature) data.

Of course, the other effect of being under way is increased vibration. The R21 light measurements taken in port have standard deviations that are approximately 40% less than that of the data collected under way. This is not completely unexpected, since ships have a large range of motion frequencies that are transmitted throughout the work spaces, and lamp filaments are sensitive to vibrations.

There is also an indication that the higher intensity bulbs produce a more variable light field: the indoor, underway medium, and high lamp levels have standard deviations that are about 3.4 times the indoor, underway low lamp values. The larger variance in the high lamp level is probably due to the high intensity bulbs. Since the two lamp sets are interspersed, a low intensity bulb has high intensity bulbs as its neighbors. The hotter temperatures around the high intensity lamps could have a negative performance impact on the lower intensity lamps.

The dependence of variance as a function of intensity is also seen spectrally. The light output of the SQM is smallest in the blue part of the spectrum and largest in the red; the standard deviations in the radiometer signals are also smallest in the blue and largest in the red. If the $\sigma$ values are normalized by the mean signal levels (with the dark levels removed), the normalized standard deviations (also known as the coefficient of variance), $\varsigma$, are largest in the blue and smallest in the red. If the low lamp standard deviations in Fig. 2a are used as an example, the $\varsigma$ values on average range from less than 0.4% in the blue and less than 0.3% in the red.

The general conclusions regarding environmental sensitivities are also seen in the SQM internal monitor data. Figure 3 is a plot of the standard deviations for each monitor. Higher measurement variances are associated with outdoor measurements and higher intensity illuminations (medium and high). The smallest variances occurred during indoor use of the SQM at the low lamp level. Interestingly, the heater tests on SDY 298 did not produce a significantly different variance in the SQM monitor data.

Although the results considered so far are the product of investigating only one radiometer, R21, the other radiometers lead to similar conclusions. There are several ways to summarize the data from the other radiometers. The approach taken here is to calculate the mean $\varsigma$ value,

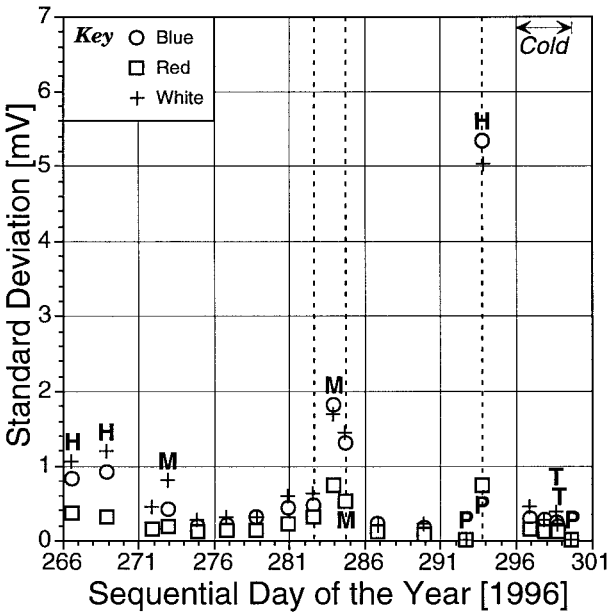


FIG. 3. The standard deviation in the internal SQM monitor voltages during all of the DAS events for R21 in Fig. 1.

$\overline{\varsigma}(\lambda_i)$, for each radiometer channel, $\lambda_i$, at a particular SQM intensity for the entire cruise. Since $\varsigma$ for a particular DAS is defined as the standard deviation of the signal divided by the mean of the signal, $\overline{\varsigma}$ is simply the temporal mean of all the $\varsigma$ values collected during all the CERT sessions. The normalization of the standard deviations allows the radiometers and channels to be intercompared.

Figure 4 is a plot of $\overline{\varsigma}(\lambda_i)$ for each channel of the eight radiometers that were used most often with the SQM during AMT-3. Several distinctive features regarding the data are immediately apparent.

1) The irradiance sensors have larger deviations than the radiance sensors; this remains true even if the channels with the largest standard deviations are discounted (as will be shown below, these seemingly errant channels have unique expressions).
2) The radiance sensors exhibit the greatest variation in the red part of the spectrum, while the irradiance sensors exhibit the greatest variation in the blue part of the spectrum.
3) The radiance and irradiance sensors have similar deviations in the red part of the spectrum, which corresponds to the peak output of the halogen lamps.

If the anomalous $\overline{\varsigma}$ values are removed from the Fig. 4 data, representative summary $\overline{\varsigma}(\lambda_i)$ values can be computed for the radiance and irradiance sensors. This summary is produced by separately averaging the radiance and irradiance normalized standard deviations for each channel (this does not introduce extra noise to the comparison because the channels are very similar, as shown in Table 2). A comparison of the resulting radiance and

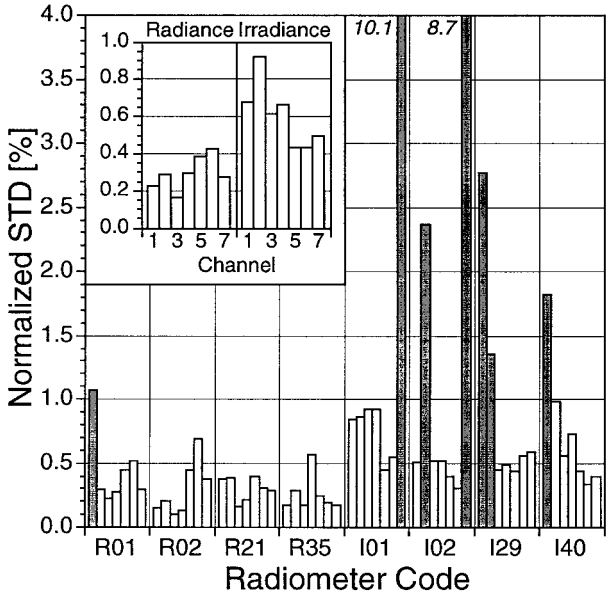


FIG. 4. The mean normalized standard deviation (STD), $\overline{\varsigma}(\lambda_i)$, for each channel of the eight radiometers used most often with the SQM during AMT-3. Channels 1–7 are plotted sequentially left to right (blue to red), and the gray bars indicate channels with (apparently) anomalously high variances. Channel 7 for radiometers I01 and I02 have such large normalized standard deviations they do not terminate on the plot, so their actual values are indicated at the top: 10.1% and 8.7%, respectively. The inset panel shows a summary of the radiance and irradiance $\overline{\varsigma}(\lambda_i)$ values with the anomalous channels (gray bars) removed from the data. This summary is produced by separately averaging the radiance and irradiance normalized standard deviations for each channel.

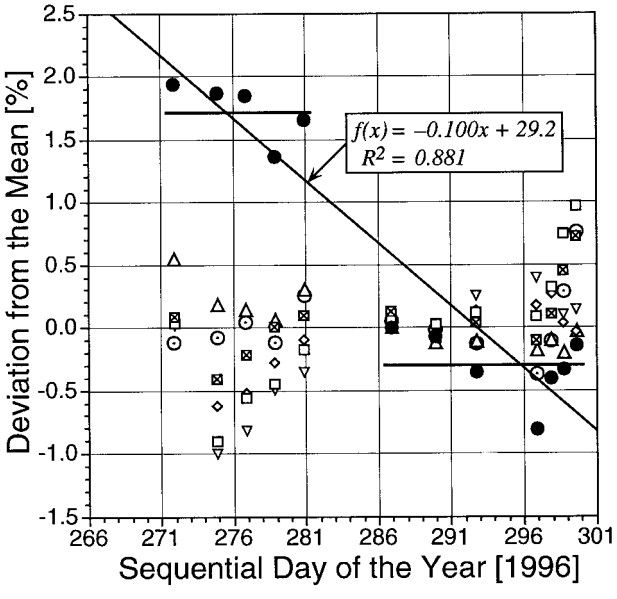


FIG. 5. A plot of $\check{L}_W^{R01}(\lambda_i)$ as a function of time. The channel coding is the same as for Fig. 1 except channel 1 is shown as a solid circle to emphasize it in the plot.

irradiance values is shown in the inset panel of Fig. 4. In a channel-by-channel comparison, the irradiance channels have a larger normalized standard deviation than the corresponding radiance channels, although all of the values are less than 1%. The larger deviations in the irradiance sensors are not unexpected because of the lower flux in the blue portion of the spectrum (lower signal to noise), the inherently higher noise of irradiance sensors (from the higher gain resistors in these instruments), and the greater sensitivity of irradiance sensors to positioning errors. The blue irradiance channels are approximately 75%–90% lower than that of the corresponding radiance channels, so variations in SQM flux will represent a larger percentage of the signal. In other words, the signal-to-noise ratio is smaller in the blue part of the spectrum. Note that the deviations in the red channels of both types of sensors are approximately equal.

To investigate the channels with anomalously high variances in Fig. 4, the radiometers involved are considered in greater detail. Figure 5 is a plot of $\check{L}_W^{R01}(\lambda_i)$ as a function of time. The anomalous temporal behavior of channel 1 is clearly evident. The question arises whether or not the temporal degradation is best modeled as a linear degradation (shown on the plot as a 0.1% per day decrease) or as a stepwise 2.04% change between one group of data for SDY 271–281 and a second group for SDY 286–301. The linear decay model has residuals that are 9.3 times larger than the stepwise model for the first group of data (271–281) and residuals that are 3.1 times larger for the second group of data.

Clearly, the 5-day period between SDY 281 and 286 was an important time to make a low lamp-level measurement with R01, but this was a time period when outdoor tests and alternative lamp-level measurements were being conducted. Unfortunately, there was an insufficient amount of time to make enough measurements at the alternative lamp levels to unequivocally choose between a linear or stepwise degradation. Discriminating between these two possibilities points to one of the difficulties associated with monitoring the performance of a radiometer—that is, determining how frequently to make the measurement. With a device capable of multiple intensities, there is also the difficulty of choosing how often to make measurements at alternative intensities. In general, utilizing only one intensity level should be adequate, but the advantage of multiple intensities is that it permits a broader range of the detector's response to be analyzed.

Channel 7 of radiometer I01 showed the greatest measurement variance during the AMT-3 deployment. The time evolution of $\check{L}_W^{I01}(\lambda_i)$ is shown in Fig. 6. Note that channel 7 changes at the rate of $-1.71\%$ per day with respect to the mean over the SDY 271–287 time period; after that, the radiometer was basically stable. Unfortunately, after SDY 293 no additional measurements with I01 could be made because of a problem with the electrical connector on the radiometer: the pins were manufactured too long and steadily deteriorated during

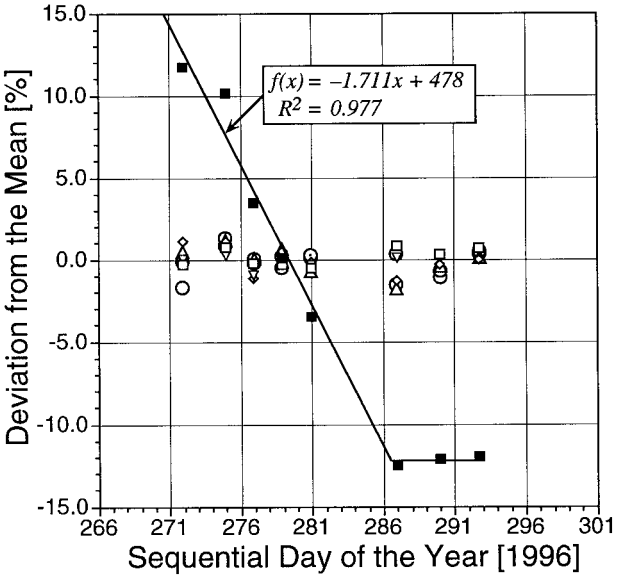


FIG. 6. The time evolution of $\check{L}_W^{I01}(\lambda_i)$. The channel coding is the same as for Fig. 1 except channel 7 is shown as a solid square to emphasize it in the plot.

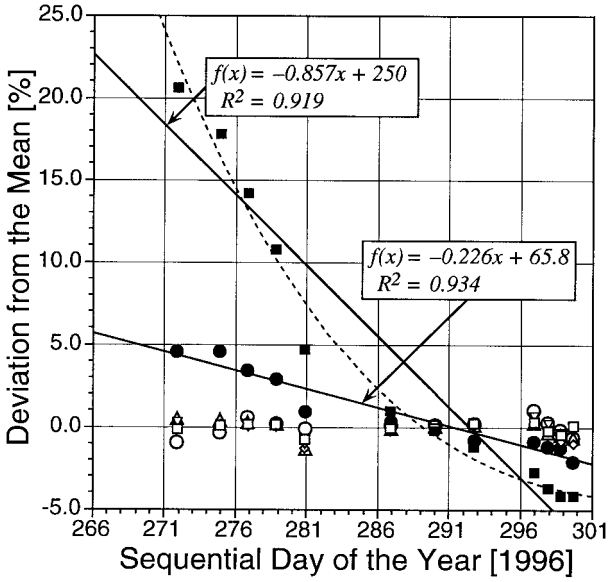


FIG. 7. A plot of $\check{L}_W^{I02}(\lambda_i)$ as a function of time. The channel coding is the same as for Fig. 1 except channels 2 and 7 are shown as a solid circle and solid square, respectively, to emphasize them in the plot. The dashed line is an alternative third-order polynomial fit to the channel 7 data.

AMT-3 until they started breaking off on SDY 294. This illustrates another difficulty with making monitoring measurements; the equipment is disconnected and reconnected many more times than usual, which increases the likelihood of cabling mistakes or failures. Under these circumstances, rugged connectors that are easy to disconnect and then reconnect are an important design requirement.

Channels 2 and 7 of I02 also showed large measurement variances. Figure 7 is a plot of $\check{L}_W^{I02}(\lambda_i)$ as a function of time. Channel 2 shows a linear decrease of 0.23% per day, while channel 7 shows a more complicated behavior. A linear fit to the channel 7 data indicates a decrease of 0.86% per day. A third-order polynomial fits the data better and has residuals with respect to the fitted curve that are 2.4 times smaller than the residuals for the linear fit. Additional SQM data was collected approximately 65 days after AMT-3. These data show a continuing decrease in channels 2 and 7 for this radiometer. Using the mean established during AMT-3, channels 2 and 7 were 12.62% and 30.29% below the mean when the final measurements were made. Although these reductions are not as large as the linear fits to the AMT-3 data would predict, they are substantially in the correct direction and point to the continued deterioration of these channels. In comparison, channels 1, 3, 4, 5, and 6 after the cruise were −1.88%, 0.31%, 0.37%, 0.08%, and 0.41% with respect to the AMT-3 mean, respectively.

The fits to the individual channels considered in Figs. 5–7 suggest suitable corrections to the response of anomalous channels can be constructed. This is true as long as the temporal sampling with the SQM is in keeping with the errant behavior of the channel involved. If the poor performance of a particular channel is simply the result of a large increase in (seemingly) random noise, little can be done except to increase the number of observations. Unfortunately, the anomalous channels of radiometers I29 and I40 during low lamp-level illumination fall into this latter category—the channels involved are simply noisier and there is no evidence of a deterministic degradation of the signal. Upon inspection of the signal levels associated with the low, medium, and high lamp levels, the most likely source of this noise is inadequate flux at the low lamp level. At the low lamp level, the irradiance blue channels are operating just above their dark levels, so even small inhomogeneities in the light field can be significant with respect to the mean. A comparison of the irradiance sensors at the medium lamp levels, for example, shows the mean normalized standard deviation for each channel is less than 0.5% if the errant channels analyzed in Figs. 5–7 are excluded from the analysis.

The temporal stability of the SQM itself, both in terms of the generated light field and the internal monitors, is the last item addressed here. Figure 8 is a time series of the three fiducials used during low lamp-level illuminations, as measured by the white SQM monitor. Each data point is the percent deviation of the monitor signal, with respect to the mean, for that particular fiducial and CERT session. Since several minutes of data or several DAS events were collected during each CERT session, each data point is usually a mean for a particular CERT session. The data clearly shows a steady degradation in the low lamp-level intensity. Using all of the fiducials, a least squares linear fit yields a degradation rate of

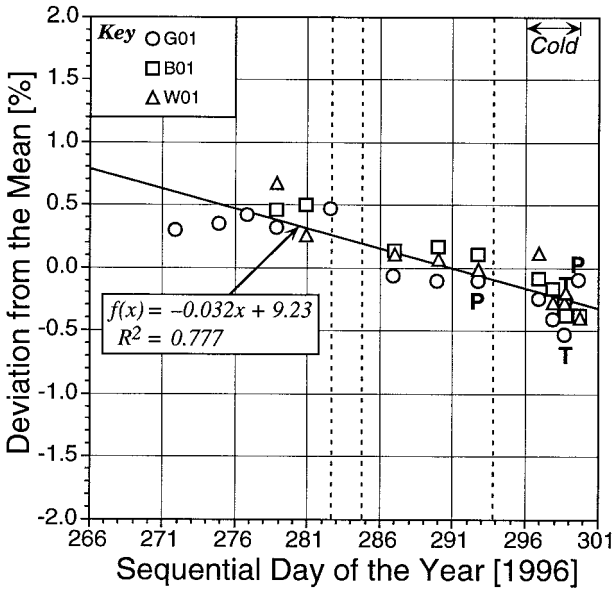


FIG. 8. A time series of the three fiducials used during low lamp-level illuminations as measured by the white SQM monitor. The fitted line is with respect to all of the data.

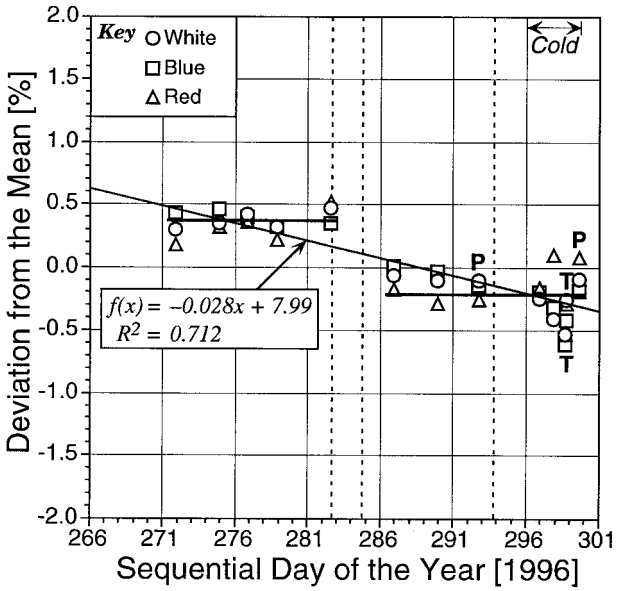


FIG. 9. A plot of the low lamp-level glass fiducial (G01) data as measured by all three internal SQM monitors. The diagonal fitted line is with respect to all of the data, whereas the two smaller horizontal lines represent mean levels for the groups of data they encompass.

about 0.03% per day; which means the SQM low lamp-level flux decreased by approximately 1.1% over the course of AMT-3.

## 6. Conclusions

To evaluate the overall capability of the SQM, the eight most frequently used radiometers (Table 1) illuminated at the low lamp level and filtered to remove any spurious channels represent the most comprehensive data. The mean normalized standard deviations, $\overline{s}(\lambda_i)$, for each channel of the radiance and irradiance sensors indicate the SQM is capable of monitoring the stability of a radiometer to within 1% (Fig. 4 inset). If all of the radiance and irradiance $\overline{s}$ values are averaged, the mean of the radiance channels is 0.30% ($\pm$0.15%) and the mean of the irradiance channels is 0.58% ($\pm$0.20%). As noted before, the larger irradiance standard deviations are probably because of the lower flux in the blue part of the spectrum and the inherently higher noise of irradiance sensors.

The limited data from the higher precision radiometers confirm the basic capabilities of the SQM. If the radiance and irradiance $\overline{s}$ values for Q16 and H23 are averaged, the mean of the radiance channels is 0.21% ($\pm$0.09%) and the mean of the irradiance channels is 0.33% ($\pm$0.27%). The normalized irradiance standard deviations are again larger than the radiance values. Including the other less frequently used radiometers, the surface reference sensors (H24 and M30) do not change this conclusion.

Since normalized results are being used here, the degradation of the SQM itself does not appear explicitly. The initial analysis of the SQM white monitor (Fig. 8) suggested a small but persistent decrease in the SQM light field. The linear degradation model may be appealing from the vantage of diffuser aging and electronic drift, but the data suggest a stepwise decay is a likely possibility. Not only is this true in terms of the fiducial data (Fig. 8), but also in terms of the radiometric data, which showed detectors can change in a number of different ways (Figs. 5–7). The internal monitors are considered the independent measure of the SQM light field, so a change in the apparent SQM flux may be partly due to a change in the monitors and not just the lamps.

The SQM is a new instrument with a limited amount of deployment data and a paucity of information regarding the decay of the lamps, the diffuser, the electronics, or the filtered monitors. Although there is an inadequate amount of medium and high intensity data to address more of the specifics about SQM aging, a closer inspection of the low lamp-level data shows the aging is spectrally similar. Figure 9 is a plot of the low lamp-level glass fiducial data (G01), as measured by all three SQM monitors. With minor variations, each monitor presents a similar description of the degradation in the SQM light field: linear fits to the individual monitor measurements yield comparable estimates of the decay rate. If the monitors are taken together as a group (rather than separately), a linear fit to all the data yields a decay rate of about 0.03% per day. This, of course, is the same value arrived at earlier utilizing the white monitor and all three fiducials (Fig. 8). Once again, however, the data suggest a stepwise change is a likely model of the temporal evolution of the SQM light field.

Separating the data into two periods, SDY 271–285 and 286–300, and then fitting the average of the monitor signals in each of those regimes, produces a stepwise model of the SQM light field decay. The residuals to the linear decay model are approximately twice as large as the stepwise model during the first time period and almost four times as large during the second. Not only does the stepwise model fit the decay in the SQM illumination better, but the stepwise change in the SQM low lamp-level during AMT-3 is only 0.58% (versus 1.1% for the linear decay model). Given the low lamps were used for approximately 63 h during AMT-3, this type of change is in keeping with expectations derived from other tungsten filament lamps: an FEL, for example, is expected to change by approximately 1% for every 50 h of use.

Further evidence that the change in SQM flux was due to a change in one or more of the lamps is provided by the low lamp-level deck box data. A comparison of the eight 1-A lamps shows seven behaved very similarly and one did not. Lamps 1–7 had similar operating voltages, 3.25–3.35 V and decayed in a mostly linear fashion at a rate of 0.3–0.6 mV per day. These decay rates represent about a 0.01%–0.02% per day change in lamp voltage. Over the course of the 36-day AMT-3 deployment, then, the operating voltages of lamps 1–7 decreased by about 0.33%–0.64%. Lamp 8, however, operated at a higher voltage at all times, approximately 3.52 V, and showed an obvious stepwise change in operating voltage in keeping with the change in SQM flux: during SDY 271–285, the mean voltage was 3.525 V; and during SDY 286–300, the mean voltage was 3.509 V. This represents a 16-mV drop in operating voltage or a decrease of approximately 0.45% between the two time periods. Such a change could be because of a partial short in the bulb. Given the magnitude of the change in lamp voltage, a change in mechanical alignment—for example, a repositioning of the lamp socket assembly—is ruled out as a significant cause for the observed change in SQM flux.

The principal findings of this field commissioning are as follows.

1) The SQM can be used to track the stability of field radiometers at less than the 1% level in terms of the relative radiometric response of the instruments. This capability is mostly a consequence of the independent short-term monitoring that is provided by the internal monitors, but it is also because of the long-term stability of the generated light field, which is achieved using the computer-controlled, precision current sources.
2) The SQM light field is sufficiently stable to allow for a sensitive measure and, thus, modeling of changes in the individual channels of commercial radiometers. Of the eight primary radiometers used during AMT-3, three exhibited changes that were best characterized by linear, third-order polynomial, and stepwise temporal fits.
3) Based on the radiometers used during AMT-3, daily SQM measurements are needed to resolve the temporal changes in the response of the sensors. This is particularly true if the point in time when a stepwise change is to be determined or if a distinction between heightened noise and a temporal trend is to be made.
4) In terms of the generated light field and the internal monitors, SQM performance decayed approximately 0.6% during the course of the 36-day AMT-3 deployment. This change was expressed best as a stepwise (rather than a linear) decay, and since it was seen in all three internal monitors, it was probably because of a partial short in the output of one of the lamps. (Low lamp number 8 was shown to have a stepwise change in its operating voltage, −0.45%, that was similar to, and coincided with, the observed change in SQM performance.)

In many cases, the absolute calibration of a radiometer might occur only once or twice a year. Even if a more frequent calibration schedule were possible, the equipment involved necessarily prevents calibrations while the radiometers are being used in the field. Lacking a device like the SQM, individual radiometer channels could be corrected only from one calibration point to another without an intervening understanding of how the channels involved changed and, thus, no defensible way to choose a correction methodology. The AMT-3 SQM data clearly shows individual channels can temporally evolve in one of several different ways, some of which, like a stepwise change or a third-order polynomial, are incompatible with a simple linear fit to the calibration points.

The large magnitude in the responsivity change of some of the radiometers (as much as approximately 25% over a 1-month period) suggests a problem in the construction process of some instruments or in the quality of some of the subcomponents. Although most of the largest changes observed during AMT-3 were with irradiance sensors, at least one radiance sensor showed anomalously large changes with respect to the other radiance sensors, and there is anecdotal evidence within the ocean color community that either type of sensor can exhibit changes of this magnitude over similar timescales. It seems likely, then, that the source of the problem is common to both types of sensors. According to the manufacturer, there is nothing in the construction process that could account for changes as large as 25% over a 30-day time period.

The most likely explanation is a degradation in the filters for the individual channels. All of the UOR and SeaOPS radiometers were built with so-called *soft* filters, that is, filters manufactured with the thermal-evaporative deposition technique. In comparison, the SeaFALLS radiometers were built with so-called *hard* filters, that is, filters manufactured with the ion-deposition technique.

Interestingly, none of the SeaFALLS radiometers exhibited large responsivity changes; the individual channels all changed less than 0.5% over the course of the AMT-3 cruise. This is not a conclusive point, however, since these radiometers comprise a smaller set of instruments and CERT sessions.

Soft filters, however, are known to exhibit a larger variance in temporal stability. This is caused by a chemical deterioration of the filter, which is a function of temperature and the amount of moisture that was trapped in the filter during the manufacturing process. The former usually results in a small change over time, whereas the latter can produce more rapid changes. The variance in moisture content usually results in certain *lots* or *batches* of soft filters from a particular manufacturer exhibiting greater or lesser stability as a function of time. Unfortunately, there is no way to tell if a soft filter will decay quickly except by letting it age, so soft filters are no longer being used by Satlantic. As a result of this study (and problems with certain other radiometers), all of the UOR and SeaOPS radiometers have had their filters changed to the ion-deposition type.

*Acknowledgments.* Several individuals contributed directly or indirectly to the success of the first SQM field deployment, including P.-S. Shaw, C. Johnson, D. Lynch, and G. Moore; their efforts are gratefully acknowledged. J. Brown was responsible for much of the at-sea radiometric data acquisition capability, which was an indispensible part of the field effort. The expert seamanship of the master and crew of the RRS *James Clark Ross* is greatly appreciated. S. Maritorena, G. Eplee, C. McClain, and S. McLean provided useful review comments, and the final preparation of the manuscript benefitted from the editorial and logistical assistance of E. Firestone.

## REFERENCES

Aiken, J., and I. Bellan, 1990: Optical oceanography: An assessment of a towed method. *Light and Life in the Sea*, P. J. Herring, Ed., Cambridge University Press, 39–57.

Hooker, S. B., and W. E. Esaias, 1993: An overview of the SeaWiFS project. *Eos, Trans. Amer. Geophys. Union,* **74,** 241–246.

——, C. R. McClain, and A. Holmes, 1993: Ocean color imaging: CZCS to SeaWiFS. *Mar. Tech. Soc. J.,* **27,** 3–15.

Johnson, B. C., P.-S. Shaw, S. B. Hooker, and D. Lynch, 1998: Radiometric and engineering performance of the SeaWiFS Quality Monitor (SQM): A portable light source for field radiometers. *J. Atmos. Oceanic Technol.,* **15,** 1008–1022.

McClain, C. R., W. E. Esaias, W. Barnes, B. Guenther, D. Endres, S. B. Hooker, G. Mitchell, and R. Barnes, 1992: Calibration and validation plan for SeaWiFS. NASA Tech. Memo. 104566, Vol. 3, S. B. Hooker and E. R. Firestone, Eds., NASA/Goddard Space Flight Center, Greenbelt, MD. 41 pp. [Available from NASA Center for Aerospace Information, 7121 Standard Drive, Hanover, MD 21076-1320.]

Mueller, J. L., and R. W. Austin, 1995: Ocean optics protocols for SeaWiFS validation, revision 1. NASA Tech. Memo. 104566, Vol. 25, S. B. Hooker and E. R. Firestone, Eds., NASA/Goddard Space Flight Center, Greenbelt, MD. 66 pp. [Available from NASA Center for Aerospace Information, 7121 Standard Drive, Hanover, MD 21076-1320.]

Robins, D. B., and J. Aiken, 1996: The Atlantic Meridional Transect: An oceanographic research programme to investigate physical, chemical, biological, and optical variables of the Atlantic Ocean. *Underwater Tech.,* **21,** 8–14.

——, and Coauthors, 1996: AMT-1 cruise report and preliminary results. NASA Tech. Memo. 104566, Vol. 35, S. B. Hooker and E. R. Firestone, Eds., NASA/Goddard Space Flight Center, Greenbelt, MD. 87 pp. [Available from NASA Center for Aerospace Information, 7121 Standard Drive, Hanover, MD 21076-1320.]

Shaw, P.-S., B. C. Johnson, S. B. Hooker, and D. Lynch, 1997: The SeaWiFS Quality Monitor—A portable field calibrator light source. *Proc. SPIE,* **2963,** 772–776.

Waters, K. J., R. C. Smith, and M. R. Lewis, 1990: Avoiding ship-induced light-field perturbation in the determination of oceanic optical properties. *Oceanogr.,* **3,** 18–21.